Int. J. Heat Mass Transfer. Vol. 36, No. 7, pp. 1943–1952, 1993
Printed in Great Britain

0017–9310/93 $6.00 + 0.00

Lateral velocity fluctuations and dissipation time scale ratios for prediction of mean and fluctuating temperature fields

P. J. GEHRKE and K. BREMHORST
Department of Mechanical Engineering, The University of Queensland, QLD 4072, Australia

(*Received* 18 *March* 1992)

Abstract—Further testing of a previously developed diffusivity-based model for predicting mean and fluctuating temperatures in water and liquid sodium flows downstream of a multi-bore jet block in which one jet is heated is performed but using air as the working fluid. The apparatus used enabled geometric similitude with the previous studies. The previous model used longitudinal turbulence intensities and longitudinal integral length scales to estimate values of the eddy diffusivity of heat. Measurement of lateral velocities in the present work allowed a significant improvement to be made in the modelling procedure. It was found that the lateral turbulence intensity was a more effective velocity scale to use and a length scale based on lateral velocity fluctuations was more apt. The Prandtl number effect on temperature dissipation rates found previously in water and sodium is extended by the results using air, leading to a simple algebraic relation between the Prandtl number and dissipation time scale ratio. The non-isotropic nature of the flow is identified and is seen to influence the results.

1. INTRODUCTION

KNOWLEDGE of velocity field information at the exit plenum of fuel rod bundle sub-assemblies of sodium-cooled nuclear reactors is of importance. Local blockages in the coolant flow can lead to reduced performance and safety problems. Under operating conditions, reliable instrumentation does not exist to directly measure velocity fields. Deduction of coolant flows is thus required from another source. One possible method is to infer the velocity field from the mean and fluctuating temperature field. Temperature field data in liquid sodium can be obtained from thermocouple measurements. In order to achieve this relation, mathematical models must be employed. To reliably use such models measurements of both the velocity and temperature field are required. Controlled studies using water [1], which gives dynamic similarity, have been performed, as have direct measurements with sodium [2]. Accurate velocity measurements in these fluids are difficult; hence a more convenient working fluid, namely air, was used.

Fuel rod sub-assemblies consist of spaced rods with the cooling medium flowing through the voids. In previous studies and the present work this geometry was simulated by the use of a multi-bore jet block in a containment pipe (Fig. 1). The flow geometry is the inverse of the fuel rod bundle, but the downstream flow can be expected to be similar. It is also expected that the flow is similar to that generated by grids. The turbulence levels at the jet block exit are expected to be high. The absence of turbulence production will, however, see the rapid downstream decay of turbulence to quite low levels. In studies with grid flows it has been shown [3] that power laws are suitable for describing the decay of turbulence. The exponents of these power laws are geometry dependent and hence must be found for each respective equipment geometry used. The downstream growth of length scales also occurs with such geometries and can also be described by power laws, as can the decay of temperature fluctuations.

The mathematical model used in the present work tried to predict the downstream mean and fluctuating

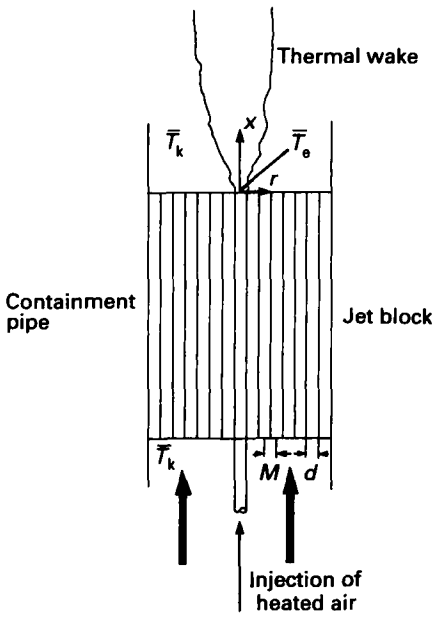

FIG. 1. Schematic of multi-bore jet block showing coordinates and flow variables.

NOMENCLATURE

a	eddy diffusivity of $\overline{\delta^2}$ [$m^2 s^{-1}$]
A, A_v, A_Λ	decay coefficients
A_u	coefficient for u'
B	proportionality constant for $\overline{\delta^2}$ decay
d	diameter of jet block bores [m]
D	containment pipe diameter [m]
$f(\hat{r})$	coefficient of spatial longitudinal velocity correlation
$g(\hat{r})$	coefficient of spatial lateral velocity correlation
L_f	longitudinal integral length scale [m]
L_g	lateral integral length scale [m]
$\hat{L}_g$	integral length scale found from transformation equation [m]
m	decay exponent for temperature fluctuation
M	jet block hole pitch [m]
n	power law exponent for eddy diffusivity
n_v	power law exponent for v
n_Λ	power law exponent for Λ
n_u	power law exponent for u'
Pr	Prandtl number
q^2	twice the instantaneous turbulent energy [$m^2 s^{-2}$]
r	radial coordinate [m]
$\hat{r}$	correlation separation distance [m]
R	dissipation time scale ratio
Re_M	Reynolds number based on velocity in bore and mesh size
S	volume flow rate of heated jet [$m^3 s^{-1}$]
t	time
$\bar{T}$	mean temperature [K]
$\bar{T}_c$	mean temperature of heated jet at jet block exit [K]
$\bar{T}_k$	mean temperature of unheated fluid [K]
u	velocity fluctuation in the x-direction [$m s^{-1}$]
u_i	velocity fluctuation in the i-direction [$m s^{-1}$]
$\bar{U}$	mean streamwise velocity [$m s^{-1}$]
$\bar{U}_i$	mean velocity in the i-direction [$m s^{-1}$]
U	instantaneous longitudinal (streamwise) velocity [$m s^{-1}$]
v	velocity fluctuation in the r-direction [$m s^{-1}$]
V	instantaneous lateral velocity [$m s^{-1}$]
x	streamwise coordinate [m]
x_i	coordinate in the i-direction [m]
x_0	effective origin for α_E [m]
x_{0v}	effective origin for v [m]
$x_{0\Lambda}$	effective origin for Λ [m]
x_{0u}	effective origin for u' [m].

Greek symbols

α	molecular diffusivity of heat [$m^2 s^{-1}$]
α_E	eddy diffusivity of heat [$m^2 s^{-1}$]
$\alpha_E(x)$	eddy diffusivity of heat as a function of x [$m^2 s^{-1}$]
δ	stream temperature fluctuation [K]
δ'_{m0}	maximum r.m.s. temperature fluctuation [K]
ε	dissipation rate of velocity fluctuations [$m^2 s^{-3}$]
ε_δ	dissipation rate of temperature fluctuations [$K^2 s^{-1}$]
Λ	characteristic turbulent length scale [m]
v	characteristic turbulent velocity [$m s^{-1}$]
π	3.14...

Subscripts

i	coordinate directions 1, 2 and 3
m	maximum value at a given axial location.

Superscripts

$\bar{}$	time average
$'$	r.m.s. value.

temperature profiles; hence the diffusive properties of the flow had to be established. For the mean temperature field, an eddy diffusivity approach was used. The fluctuating temperature field was solved by the use of a gradient diffusion model and dissipation time scale ratio.

Previous work [1, 2] used less refined but similar models to enable the prediction of mean and fluctuating temperature fields in water and sodium flows. The present work has extended this to measurements in air, thus giving a further check of Prandtl number effects. Also, only longitudinal measurements of velocity fluctuations were previously possible. With air, measurements of longitudinal and lateral components were possible, enabling the development of a more realistic diffusivity model. Extension of the present work to other liquid metal flows such as flow in dies during metal casting should be possible.

2. MATHEMATICAL MODEL

The coordinate system and flow variables are shown in the schematic diagram (Fig. 1). The model is based on the diffusion of heat emanating from the central bore and assumes that the resultant thermal wake of interest does not extend sufficiently in the radial direction to be influenced by any boundary layer which forms on the containment pipe wall.

For the mean temperature field, the energy equation is used. Assuming a steady state, incompressible flow with negligible heating from dissipation and no internal heat sources, the equation reduces to

$$\bar{U}_i \frac{\partial \bar{T}}{\partial x_i} = \frac{\partial}{\partial x_i}\left[\alpha \frac{\partial \bar{T}}{\partial x_i} - \overline{u_i \delta}\right], \tag{1}$$

where the Einstein summation convention applies to repeated indices. For the jet block, $\bar{U}_2 = \bar{U}_3 = 0$ except at the immediate exit of the bores. The last term of equation (1) can be modelled by the Boussinesq or gradient diffusion approximation, equation (2), to obtain equation (3):

$$\overline{u_i \delta} = -\alpha_E \frac{\partial \bar{T}}{\partial x_i} \tag{2}$$

$$\bar{U}_i \frac{\partial \bar{T}}{\partial x_i} = \frac{\partial}{\partial x_i}[\alpha + \alpha_E]\frac{\partial \bar{T}}{\partial x_i}. \tag{3}$$

For both of these equations, α_E is assumed to be a scalar at a given downstream position. The use of a turbulent Prandtl number to find a value of the eddy diffusivity of heat from the eddy diffusivity of momentum is not possible as a radial mean velocity gradient does not exist. To close equation (3), a different model must be used. Assuming that temperature is a passive scalar, a model for the eddy diffusivity of heat in terms of velocity field values can be obtained by using the Lagrangian description of diffusion, which leads to

$$\alpha_E = v\Lambda, \tag{4}$$

where v is a characteristic turbulent velocity and Λ is a characteristic turbulent length scale. In ref. [2], v and Λ were assumed to be represented by the streamwise velocity fluctuation u' and its integral length scale L_f, respectively. In the present analysis both terms will be kept in a general format. Since the flow is similar to grid flows, it will be assumed [3] that the decay of velocity fluctuations displays a power law dependence on downstream position. It will also be assumed that, as for grid flows [3], the length scale growth follows a power law allowing equations (5) and (6) to be written as

$$\frac{v}{\bar{U}} = A_v\left[\frac{x}{d} - \frac{x_{0v}}{d}\right]^{n_v} \tag{5}$$

$$\frac{\Lambda}{d} = A_\Lambda\left[\frac{x}{d} - \frac{x_{0\Lambda}}{d}\right]^{n_\Lambda}. \tag{6}$$

The terms A_v, A_Λ, n_v, n_Λ, x_{0v} and $x_{0\Lambda}$ can be obtained from experimental data. To estimate the downstream variation of α_E it is assumed that the product of v and Λ also displays a power law dependence and hence can be modelled directly as

$$\frac{\alpha_E}{\bar{U}d} = \frac{v\Lambda}{\bar{U}d} = A\left[\frac{x}{d} - \frac{x_0}{d}\right]^n. \tag{7}$$

Equation (7) implies that $n = n_v + n_\Lambda$, $A = A_v A_\Lambda$ and that $x_0 = x_{0v} = x_{0\Lambda}$. Except for regions close to the jet block exit ($x/d < 10$), the velocity field is assumed to be homogeneous in the radial and azimuthal directions. Hence the eddy diffusivity is a function only of downstream direction, $\alpha_E \Rightarrow \alpha_E(x)$.

At this point in the analysis the equation for the downstream decay of u' will be written independently of equation (5) as this is required later:

$$\frac{u'}{\bar{U}} = A_u\left[\frac{x}{d} - \frac{x_{0u}}{d}\right]^{n_u}. \tag{8}$$

Equation (3) can be simplified by assuming that changes in the mean temperature are greatest in the radial direction and that α and $\alpha_E(x)$ are independent of temperature. Conversion to cylindrical coordinates yields

$$\bar{U}\frac{\partial \bar{T}}{\partial x} = [\alpha + \alpha_E(x)]\left[\frac{1}{r}\frac{\partial \bar{T}}{\partial r} + \frac{\partial^2 \bar{T}}{\partial r^2}\right]. \tag{9}$$

Using theory based on diffusion from a fixed source in a uniform flow [9], the analytical solution for equation (9) for points where $x/d > 5$ and $r^2 \ll x^2$ is

$$\frac{\bar{T} - \bar{T}_k}{\bar{T}_c - \bar{T}_k} \approx \frac{S}{4\pi\left[\alpha + \frac{1}{n}\alpha_E(x)\right]x} \exp\left[\frac{-\bar{U}r^2}{4\left[\alpha + \frac{1}{n}\alpha_E(x)\right]x}\right], \tag{10}$$

where S is the volume flow rate of the heated jet. The analysis allows for the fact that α_E is a function of downstream position.

Analysis of the fluctuating field starts with the steady state balance for temperature fluctuations [4]:

$$\bar{U}_i \frac{\partial \overline{\delta^2}}{\partial x_i} = -2\overline{u_i\delta}\frac{\partial \bar{T}}{\partial x_i} - \frac{\partial \overline{u_i\delta^2}}{\partial x_i} + \frac{\partial}{\partial x_i}\left(\alpha \frac{\partial \overline{\delta^2}}{\partial x_i}\right) - 2\alpha\,\overline{\frac{\partial \delta}{\partial x_i}\frac{\partial \delta}{\partial x_i}}. \tag{11}$$

Again $\overline{u_i\delta}$ is modelled by equation (2), while $\overline{u_i\delta^2}$ is modelled by the gradient diffusion approximation:

$$\overline{u_i\delta^2} = -a\frac{\partial \overline{\delta^2}}{\partial x_i}. \tag{12}$$

The diffusion coefficient a is assumed to be equal to α_E [2, 5].

To achieve closure, the last term of equation (11) must be modelled. This is the dissipation term which is modelled [6] by the introduction of the dissipation time scale ratio R to relate the dissipation of $\overline{\delta^2}$ to dissipation of turbulent kinetic energy:

$$R = \frac{\varepsilon\overline{\delta^2}}{\overline{q^2}\varepsilon_\delta}. \tag{13}$$

$2\varepsilon_\delta$ equals the dissipation term in equation (11) and R is assumed to be constant for a particular flow. Values

for R of 0.833 for grid flows and 0.5 for shear flows were given in ref. [5], while ref. [2] reported values of 0.38–0.44 and 0.75 for sodium and water jet block flows respectively. Equation (11) in its modelled form becomes

$$\bar{U}_i \frac{\partial \overline{\delta^2}}{\partial x_i} = 2\alpha_E \left(\frac{\partial \bar{T}}{\partial x_i}\right)^2 + \frac{\partial}{\partial x_i}\left[(\alpha+\alpha_E)\frac{\partial \overline{\delta^2}}{\partial x_i}\right] - \frac{2\varepsilon\overline{\delta^2}}{R\overline{q^2}}. \tag{14}$$

Simplification is possible by assuming

$$\bar{U}\frac{\partial \overline{\delta^2}}{\partial x} \gg \frac{\partial \alpha_E}{\partial x_i}\frac{\partial \overline{\delta^2}}{\partial x_i},$$

$$\frac{\partial^2 \overline{\delta^2}}{\partial x^2} \ll \frac{1}{r}\frac{\partial}{\partial r}\left(r\frac{\partial \overline{\delta^2}}{\partial r}\right)$$

and that the velocity field is isotropic, meaning

$$\overline{q^2} = 3\overline{u^2} \tag{15a}$$

and

$$\varepsilon = -\tfrac{3}{2}\bar{U}\frac{\mathrm{d}\overline{u^2}}{\mathrm{d}x}. \tag{15b}$$

Using the decay law, equation (8), for u' gives

$$\frac{\varepsilon}{\overline{q^2}} = \frac{n_u \bar{U}}{(x-x_{0u})}. \tag{16}$$

The final result in cylindrical coordinates is

$$\bar{U}\frac{\partial \overline{\delta^2}}{\partial x} = \alpha_E(x)\left[2\left(\frac{\partial \bar{T}}{\partial x}\right)^2 + 2\left(\frac{\partial \bar{T}}{\partial r}\right)^2\right] + [\alpha+\alpha_E(x)]\left[\frac{\partial^2 \overline{\delta^2}}{\partial r^2} + \frac{1}{r}\frac{\partial \overline{\delta^2}}{\partial r}\right] + \frac{2n_u \bar{U}\overline{\delta^2}}{R(x-x_{0u})}. \tag{17}$$

From velocity field measurements the decay exponent n_u and the effective origin x_{0u} are available, as is α_E, through equation (7). The boundary conditions that apply at the point $(x, D/2)$ are $\overline{\delta^2} = 0$ and $\partial\overline{\delta^2}/\partial r = 0$, where D is the containment pipe diameter. Given a starting profile, equation (17) can then be solved for $\overline{\delta^2}$ using various values of R and selecting that value of R giving the best fit to measured temperature fluctuation profiles.

3. APPARATUS AND INSTRUMENTATION

The experiments performed consisted of injecting into the centre bore of the jet block a heated flow of air and measuring the required parameters downstream. Similar experiments using water and sodium as the working fluid have been performed and are described in refs. [1] and [2]. To enable similitude with these results, the jet block was geometrically similar. It consisted of 158 bores of 8.7 mm diameter on a triangular pitch of 9.9 mm. The length-to-diameter ratio was 17.1:1 and the blockage ratio (non-flow area relative to total area) was 32.5%. The jet block was housed in a containment pipe of 133 mm diameter which was large enough to avoid any interaction between the heated jet and the boundary layer forming on the containment pipe wall. To avoid asymmetry due to any buoyancy effects, a vertical wind tunnel was used with heated air from a separate source being injected into the centre bore. This flow was controlled to ensure minimal velocity mismatch between the heated and ambient bores. Figure 2 shows a schematic diagram of the experimental rig.

To enable the simultaneous measurement of the U and V velocities, a DISA X-Probe Type 55P51 was used with 5 μm Wollaston wire. An active wire length of approximately 1 mm was used. For the simultaneous measurement of stream temperature, a single wire set of prongs was attached to the X-probe, attached to which was a 2.5 μm Wollaston wire with an active length of 1 mm. To resolve the velocity wire voltages, two DISA 55 M01 main units with 55 M11 CTA booster adaptors were employed. The wires were operated with a resistance ratio of 1.3. The temperature wire voltage was obtained using a 55 M20 constant current bridge. This bridge was modified for temperature fluctuation measurements [7]. The wire current used was low enough to ensure the sensor was insensitive to the fluid velocity. The method of signal

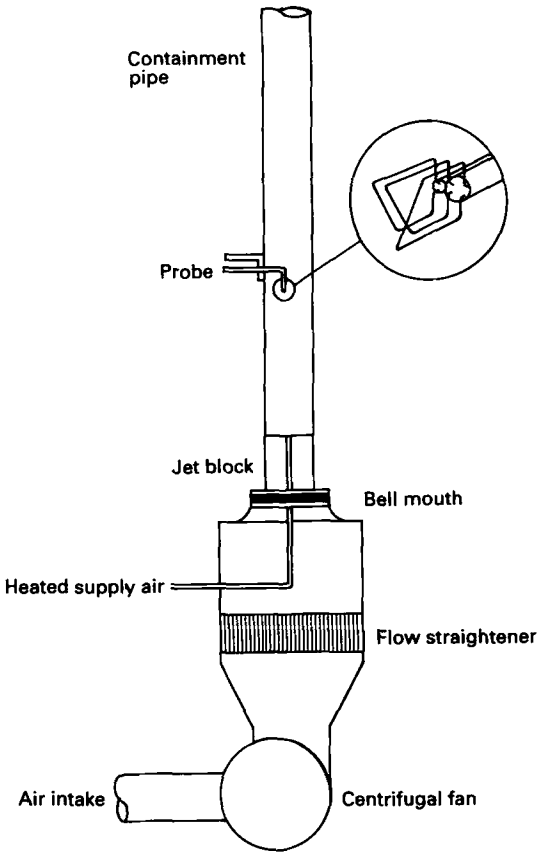

FIG. 2. Schematic diagram of experimental apparatus.

separation and processing to yield velocity and temperature data was as described by Bremhorst and Graham [8]. The temperature wire response had to be considered in order to measure correctly temperature fluctuations occurring at a frequency greater than the corner frequency of the wire. The method developed in ref. [8] requires dE_W/dt (where E_W is the temperature wire voltage) to be found. This was evaluated by fitting a natural cubic spline to seven consecutively measured voltages and taking the derivative. The resulting equation is

$$\frac{dE_{Wi}}{dt} = \frac{1}{h}\left[\frac{E_{Wi+3}}{30} - \frac{E_{Wi+2}}{5} + \frac{4E_{Wi+1}}{5} - \frac{4E_{Wi-1}}{5} + \frac{E_{Wi-2}}{5} - \frac{E_{Wi-3}}{30}\right], \quad (18)$$

where h is the time between samples (h = constant (s)) and E_{Wi} corresponds to the ith consecutively sampled temperature wire voltage. Measurements using the three-wire probe could be taken at specific downstream positions over a range of radial points using a traversing mechanism. A diagrammatic representation of the probe is included in Fig. 2.

4. EXPERIMENTAL AND THEORETICAL RESULTS

To obtain similitude with the results of Bremhorst *et al.* [2] and Krebs *et al.* [1], the experiments were performed at a similar Reynolds number (Re_M). Bremhorst *et al.* [2] used $Re_M = 17{,}070$, while the present work was performed at $Re_M = 18{,}250$. The ambient air temperature (T_k) averaged 297 K, while the centre bore temperature (T_c) remained at 312.5 K during the course of the experiments. This gave a temperature deficit of 15.5 K.

Equation (10) was used to determine the downstream decay of the centreline mean temperature. An expression for $\alpha_E(x)$ was required (equation (7)). Previous researchers had used u' ($v = u'$) and the integral length scale based on $u(\Lambda = L_f)$ to obtain a value for n. The quantity A was selected to give the best fit to the experimental temperature decay data. L_f and u' were used in the present analysis but both n and A were found purely from velocity data. This resulted in predictions for the mean temperature decay that were too low compared with the experiments. Results could be improved for $x/d > 20$ by increasing the effective origin x_0/d to a value of 10, which gave values of $A = 0.0131$ and $n = -0.220$ in equation (7). The use of $x_0/d = 10$, however, was not experimentally justifiable as it was larger than the measured effective origin. The lateral velocity fluctuation v' and the integral length scale based on lateral velocity fluctuations (L_g) were then used to model $\alpha_E(x)$. The resulting expression (from equation (7)) is

$$\frac{\alpha_E}{\bar{U}d} = 0.0183\left(\frac{x}{d}\right)^{-0.358}. \quad (19)$$

The parameters used in equations (5) and (6) to obtain this were $x_{0v} = x_{0\Lambda} = 0$, $A_v = 0.229$, $n_v = -0.664$, $A_\Lambda = 0.0797$ and $n_\Lambda = 0.306$. An excellent fit to the experimental temperature decay data was obtained using equation (19) to model the α_E term in equation (10). The Λ term used was determined from the integral time scale of the lateral velocity fluctuations and Taylor's hypothesis. To verify the scale used, the following isotropic transformation [9] was applied:

$$g(\hat{r}) = f(\hat{r}) + \frac{\hat{r}}{2}\frac{\partial f}{\partial \hat{r}}. \quad (20)$$

$g(\hat{r})$ was found from an equation fitted to the longitudinal autocorrelation data which corresponds to $f(\hat{r})$. If the flow is isotropic, the length scale based on $g(\hat{r})$ should be the same as that of the lateral velocity fluctuations, hence enabling a check for isotropic conditions. The resulting length scales, $\hat{L}_g$, obtained from $g(\hat{r})$ of equation (20), were used with v' data to predict the mean temperature decay, but the best predictions were high. Figure 3 shows the mean centreline tem-

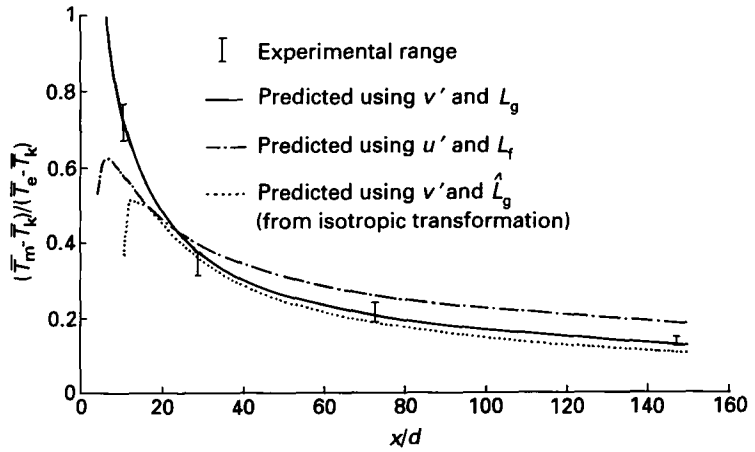

FIG. 3. Axial decay at centreline mean temperature in air.

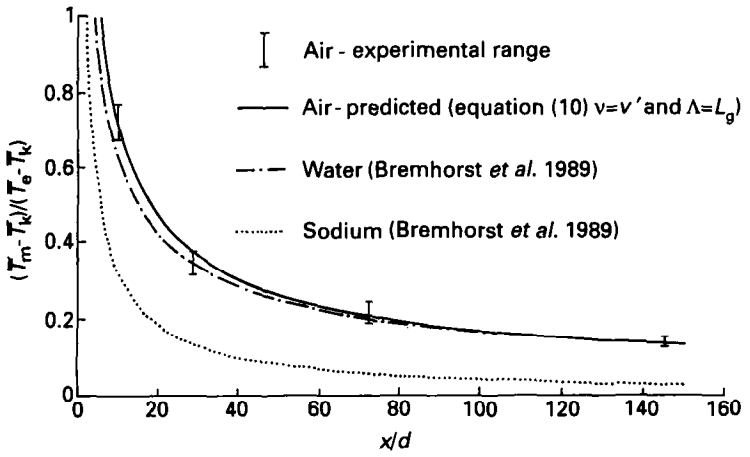

FIG. 4. Comparison of the axial decay at centreline mean temperature in different fluids.

perature curve (equation (10)) for each of the three respective sets of parameters used for ν and Λ to model α_E, plotted against an experimental range which is based on conceivable errors in the measurement of T_k and T_e. For the rest of the analysis, α_E is modelled by the quantities v' and L_g as this gave the best results. Figure 4 compares the downstream decay of the centreline mean temperature of air to those of water and sodium and demonstrates the effect of the Prandtl number.

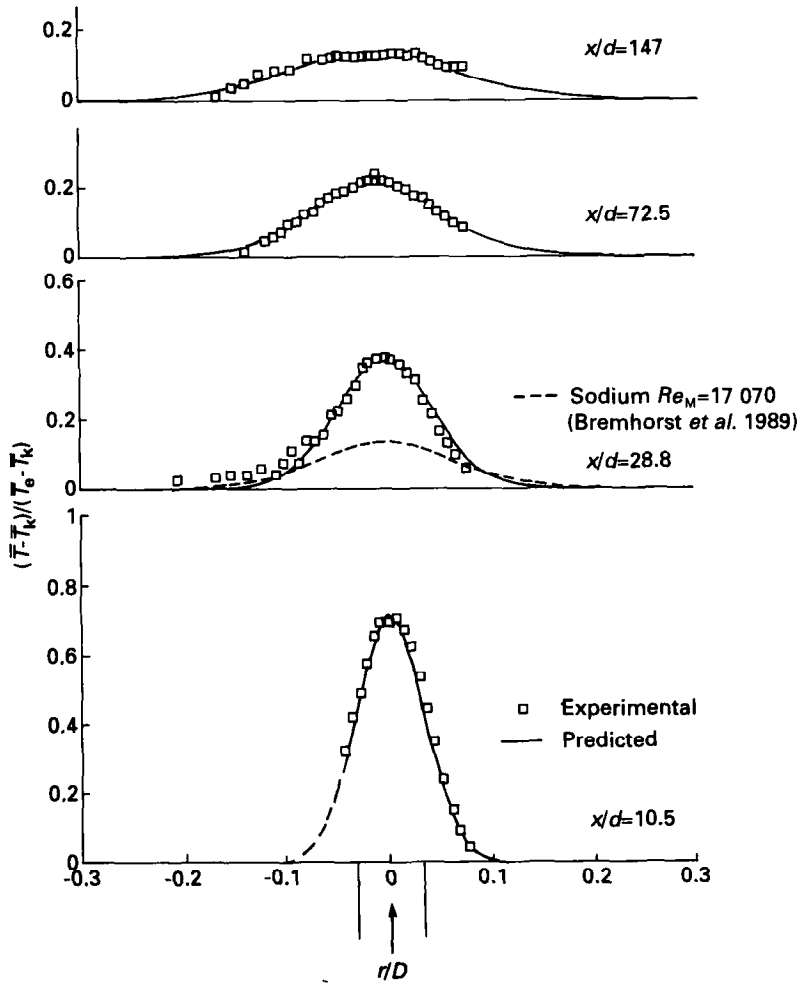

FIG. 5. Comparison of measured and predicted mean temperature radial profiles.

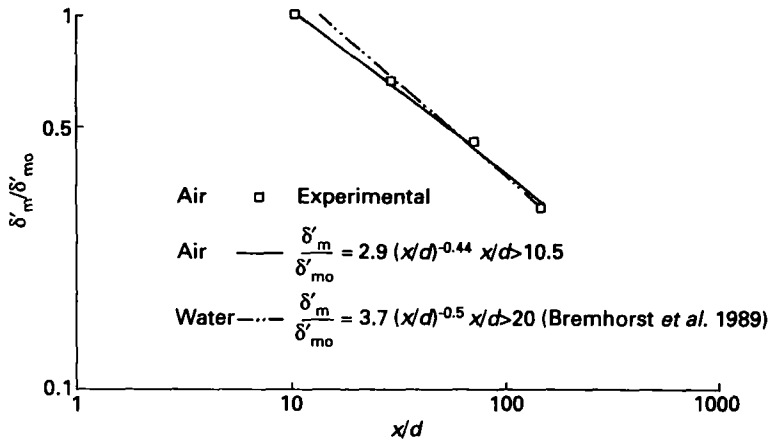

FIG. 6. Decay of temperature fluctuations in air and water.

The radial profiles could also be obtained from equation (10). Comparison of the measured and predicted profiles at specific measuring positions is shown in Fig. 5. Good agreement is observed. A comparison with the result for sodium is also included to show how significantly the Prandtl number affects mean temperature distributions once molecular diffusivity is no longer negligible.

From the experimental data obtained, the decay of temperature fluctuations was measured. The downstream decay of the maximum temperature fluctuation for each measured x/d position is shown in Fig. 6. The points can be fitted to a decay curve of the form

$$\frac{\delta'_m}{\delta'_{m0}} = B\left(\frac{x}{d}\right)^{-m}. \tag{21}$$

Figure 6 shows this curve, as well as the result for the

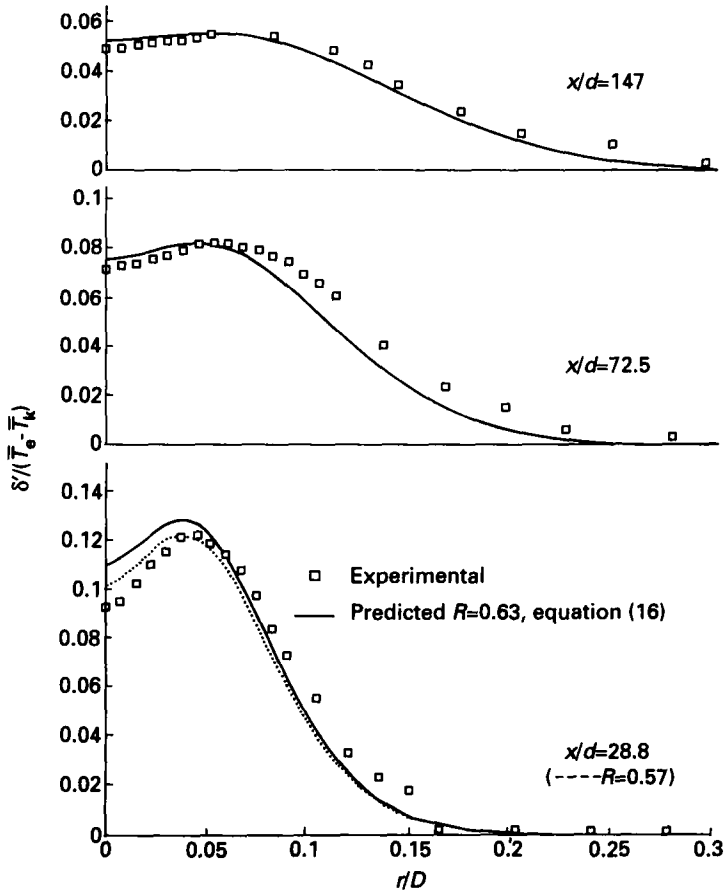

FIG. 7. Comparison of measured and predicted radial temperature fluctuation profiles.

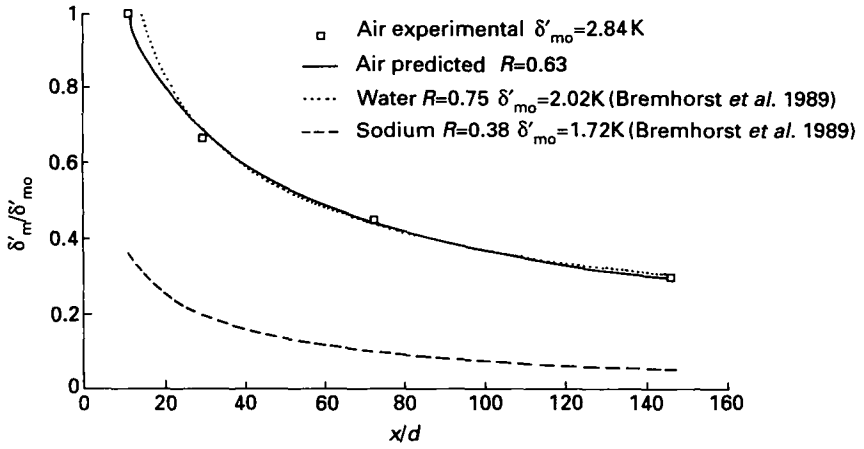

FIG. 8. Comparison of measured and predicted downstream temperature fluctuation decay.

fluctuation decay in water. The two results are seen to be quite similar but a small Prandtl number effect cannot be excluded.

To obtain theoretical profiles of the temperature fluctuations, equation (17) was solved numerically. This involved using the measured temperature fluctuation profile at $x/d = 10.5$ and solving for downstream positions using various values for the dissipation time scale ratio R. The value of R giving the best overall fit could be found. The result of this procedure is shown in Fig. 7 with satisfactory agreement between the measured and predicted values evident. Due to symmetry of points only half profiles are shown. The downstream decay of the peak temperature fluctuations was also calculated (Fig. 8), giving excellent agreement. Experimental results for water and sodium are shown for comparison with respective values of R and δ'_{m0} given.

The turbulent decay exponents had values of 1.01 and 1.06 for the downstream decay of u'^2 and v'^2, respectively. It was found that the ratio of lateral to longitudinal velocity fluctuations was between 0.60 and 0.85 over the entire measured flow regime, with an average of 0.73.

Using the value of the dissipation time scale ratio for air and the values for sodium and water supplied from Bremhorst *et al.* [2], it was possible to determine a functional relationship between R and the Prandtl number. Figure 9 gives a comparison between previous results for water and sodium flows [2] and the present one. The regression curve, equation (22), provides a good fit to the experimental data points:

$$R = 0.65(Pr)^{0.072}. \tag{22}$$

5. DISCUSSION OF RESULTS

The critical step in the modelling process is the determination of the eddy diffusivity of heat. Previous work had successfully used the method of equation (7) to achieve this but required direct determination of the constant A in equation (7). Since the X-probe technique allowed realization of lateral velocity scales the effect of using v' as the velocity scale in equation

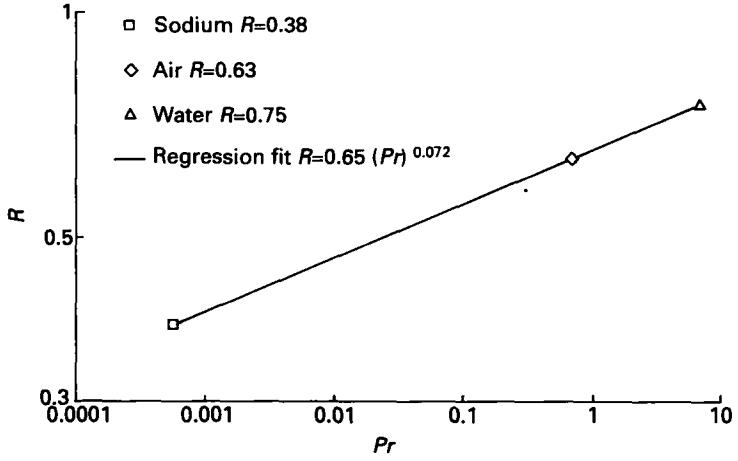

FIG. 9. Dissipation time scale ratio and fluid Prandtl number relation.

(7) was achieved. Also, the accuracy of the hot-wire technique permitted the determination of the coefficient A directly from experimental velocity data. It was seen (Fig. 3) that better results were obtained using v' rather than u'. This result endorses intuitive reasoning that diffusive processes in the lateral direction are mainly a function of the lateral fluctuating velocity. An attempt was made to check the lateral scale used by transforming the longitudinal length scale into a lateral scale using equation (20). The predictions for mean temperature based on this, however, were slightly high compared to the experimental results (Fig. 3). Equation (20) assumes isotropic flow which did not exist in the current work ($u' \neq v'$) and it was thought this effect caused an error in the calculation of $g(\hat{r})$ from equation (20). The remainder of the results were calculated using v' and L_g to model α_E.

The velocity field data compared well with those of other experimenters. The decay exponents for u'^2 and v'^2 of 1.01 and 1.06, respectively, compared well with those given by Comte-Bellot and Corrsin [3] of 1.18–1.39 for longitudinal decay behind grid flows. For water and sodium, values of 1.67 and 1.14, respectively, were found by Bremhorst *et al.* [2]. Listijono [10] found longitudinal and lateral decay exponents for air flows behind a multi-bore jet block of 1.104 and 1.152, respectively, which also compare well. Listijono also found that the ratio v'/u' was approximately 0.8 over most of the flow, which is in the range of the present measurement of 0.73 for this ratio.

Figure 4 displays the Prandtl number effect between the fluids. The curves for water and air with Prandtl numbers of 7.01 and 0.7 differed little, while sodium ($Pr = 0.0058$) was lower. This displays the much higher effect of molecular diffusion in liquid sodium. For the air and water analysis molecular diffusion was neglected. This is further highlighted in a comparison of radial profiles (Fig. 5). It can be seen that the sodium profile shown exhibits a wider radial spread than the air.

In the fluctuating temperature field analysis the profile at $x/d = 10.5$ was used as the starting point in the solution of equation (17). Values of R in the range of 0.57–0.63 provided satisfactory fits to the downstream experimental profiles with $R = 0.63$ being the optimal choice. For the prediction of the downstream decay of maximum temperature fluctuations this R value was used. As with the downstream mean temperature decay, the fluctuating decay of air and water is similar while sodium has a greater decay rate.

The terms of equation (17) were also calculated directly from all the experimental data to obtain the R values. This method entailed using the entire range of experimental data for the mean and fluctuating temperature field to evaluate the terms $\partial\overline{\delta^2}/\partial x$, $\partial\bar{T}/\partial x$, $\partial\bar{T}/\partial r$, $\partial^2\overline{\delta^2}/\partial r^2$ and $\partial\overline{\delta^2}/\partial r$ to solve for $\overline{\delta^2}$ in equation (17). This resulted in values of the dissipation time scale ratio ranging from 0.59 to 0.68. These are slightly higher than the previous method but are a good result considering that the errors in modelling some of the terms in equation (17) from the experimental profiles would have been high. Generally the values for R obtained compare well with those of other experimenters. The values recommended by ref. [5] of 0.833 for grid flows and 0.5 for shear flows agree well. The value of 0.38 for sodium and 0.75 for water jet block flows [2] are of similar magnitude and together with the present results clearly show a Prandtl number dependence of R (Fig. 9).

The sensitivity of δ' predictions based on the R value used is high. As an example, by doubling the value of R the peak δ' value at $x/d = 72.5$ is increased by 50% and decreased by 34% when R is halved. Similar sensitivities in water and sodium were found by Bremhorst *et al.* [2]. The finding of Warhaft and Lumley [11] should also be considered. They showed that temperature fluctuation decay parameters not only depended on geometry but also on the heating method. Hence R can be expected to be a function of not only the Prandtl number but also of the method of heating.

6. CONCLUSION

Using velocity field data it has been possible to model the downstream mean temperature field of a multi-bore jet block with the centre bore heated. In the estimation of the eddy diffusivity it was found that the lateral velocity fluctuation was a better velocity scale to use than the longitudinal. It was also shown that the integral length scale found from lateral velocity fluctuations was the best length scale to use.

The temperature fluctuation calculations provided values of the dissipation time scale ratio which could be compared to other work. For air, values in the range 0.57–0.63 were obtained, which compares with values for water and sodium of 0.75 and 0.38, respectively, [2]. This trend was also displayed in mean and fluctuating temperature measurements. It would be expected that the air and water cases would agree closely as in these fluids molecular diffusion effects are almost negligible. A functional relationship between the dissipation time scale ratios and Prandtl number is given.

REFERENCES

1. L. Krebs, K. Bremhorst and U. Müller, Measurement and prediction of the mean and fluctuating temperature field downstream of a multi-bore jet block in which one jet is heated, *Int. J. Heat Mass Transfer* **24,** 1305–1312 (1981).
2. K. Bremhorst, L. Krebs, U. Müller and J. B. H. Listijono, Application of a gradient diffusion and dissipation time scale ratio model for prediction of mean and fluctuating temperature fields in liquid sodium downstream of a multi-bore jet block, *Int. J. Heat Mass Transfer* **32,** 2307–2046 (1989).
3. G. Comte-Bellot and S. Corrsin, The use of a contraction to improve the isotropy of grid-generated turbulence, *J. Fluid Mech.* **25,** 657–682 (1966).

4. S. Corrsin, heat transfer in isotropic turbulence, *J. Appl. Phys.* **23,** 113–118 (1952).
5. P. Bradshaw, T. Cebeci and J. H. Whitelaw, *Engineering Calculation Methods for Turbulent Flow.* Academic Press, New York (1981).
6. D. B. Spalding, Concentration fluctuations in a round turbulent jet, *Chem. Engng Sci.* **26,** 95 (1971).
7. K. Bremhorst and L. Krebs, Reconsideration of constant current hot-wire anemometers for the measurement of fluid temperature fluctuations, *J. Phys. E: Instrum.* **9,** 804–806 (1976).
8. K. Bremhorst and L. J. W. Graham, A fully compensated hot/cold wire anemometer system for unsteady flow velocity and temperature measurements, *Meas. Sci. Technol.* **1,** 425–430 (1990).
9. J. O. Hinze, *Turbulence.* McGraw-Hill, New York (1975).
10. J. B. H. Listijono, Velocity fields behind a multi-bore jet block, M.Engng Sci. Thesis, University of Queensland, St Lucia, Australia (1985).
11. Z. Warhaft and J. L. Lumley, The decay of temperature fluctuations and heat flux in grid generated turbulence, *Symposium on Turbulence*, Technical University, Berlin, 1–5 August 1977, *Lecture Notes in Physics* No. 76 (Edited by H. Fiedler), pp. 113–123. Springer, Berlin (1978).